South African Journal of Chemical Engineering 50 (2024) 388–403

Contents lists available at ScienceDirect

South African Journal of Chemical Engineering

journal homepage: www.elsevier.com/locate/sajce

Methods used in the identification and quantification of micro(nano) plastics from water environments

Caglar Berkel , Oguz Özbek *

Tokat Gaziosmanpasa University, Faculty of Science and Arts, Department of Molecular Biology and Genetics, 60250, Tokat, Turkey

ARTICLE INFO

Keywords:
Environmental pollution
Micro(nano)plastics
Water pollution
Public health
Spectroscopy
Chromatography

ABSTRACT

Micro(nano)plastics (MNPs) pollution, which has currently become a serious environmental problem, poses a great risk to ecosystem health and biodiversity. The adverse effects of MNPs in different characteristics on organismal homeostasis are intensively studied due to their considerable threats to ecology and human/public health, since they have been identified in human blood, placenta and breast milk. To date, many studies have been carried out on MNPs, and remarkable results have been reported on their diversity, distribution, origins and their influences at the cellular level, to name a few. The literature suggests that the extent of the risk caused by MNPs is increasing significantly every year, making it even more critical and urgent to combat MNPs pollution in the environment including aquatic environments. Therefore, it is highly important to identify, quantify and monitor MNPs, especially in the water environments since it represents one of the main transportation routes of MNPs. In this review, we provide a broad and critical overview of the different methods, such as Fourier transform infrared spectroscopy (FT–IR), Raman spectroscopy, transmission/scanning electron microscopy (TEM/SEM), and gas chromatography–mass spectrometry (GC–MS), currently used in the identification and quantification of MNPs, especially in aquatic environments such as seawater and marine sediments. Each of these previous methodologies has its own unique advantages and limitations; besides, there is no validated and standardized analytical method for MNPs determination, implying that more than one method or the combinations of different methodologies are required to obtain accurate data at the current state. Moreover, considering the presence of high variability of data among different methods, more research is needed to develop a universal analytical protocol to increase reproducibility and robustness of the findings on MNPs contamination in the environment, in order to increase the credibility and impact of the field.

1. Introduction

In 2004, Thompson and his colleagues identified micro(nano)plastics that are smaller than 5 mm, causing environmental pollution (Thompson et al., 2004). Subsequently, Andrady classified plastic particles smaller than 5 mm into medium plastics (500 μm to 5 mm), microplastics (MPs) (50–500 μm), and nanoplastics (NPs) (<50 μm) according to their sizes (Andrady, 2011). Oliveira et al. classified plastics according to their sizes as nanoscale plastics (<100 nm), submicron plastics (100 nm–1 μm), and microplastics (1 μm–5 mm) (Wang et al., 2023). It takes centuries for plastics to reach these small sizes in nature, unless they are primarily produced especially in these sizes. There has been a significant increase in research on nanoplastics, which has recently became a serious environmental and public health problem (W. Liu et al., 2024). MNPs can originate from drugs, cosmetics, clothing and all other plastic products (Fig. 1) (Yu et al., 2024).

Microplastics are divided into diverse classes according to their chemical composition: polyethylene (PE), polystyrene (PS), polypropylene (PP), polyurethane (PU), polyvinyl chloride (PVC), polyamide (PA), polyester (PES), poly methyl-methacrylate (PMMA), polyamide-6 (PA6), poly-vinyl-alcohol (PVA), polybutylene terephthalate (PBT) and polyethylene terephthalate (PET), to name a few (He et al., 2022).

Plastics have a wide use in the modern daily life due to their flexibility, lightness, water resistance, low cost and stability (Huang et al., 2021; Liu et al., 2022). Based on these advantages, plastics are encountered in many areas including transportation, construction, medicine, automotive, agriculture and packaging industries (Rodrigues et al., 2019). A single plastic material can break down and turn into millions of microplastic particles. Plastic garbage and debris from

* Corresponding author.
E-mail addresses: caglar.berkel@gop.edu.tr (C. Berkel), oguz.ozbek@gop.edu.tr (O. Özbek).

https://doi.org/10.1016/j.sajce.2024.09.010
Received 19 August 2024; Received in revised form 15 September 2024; Accepted 26 September 2024
Available online 26 September 2024

Fig. 1. Sources of micro(nano)plastics.

marines drift into the oceans and slowly break down into smaller particles (Yurtsever, 2023). Today, microplastics cannot be easily purified from wastewater due to their sizes. For this reason, they can easily mix with river, lake and sea waters. In recent years, microplastic production has increased significantly, and MP concentrations detected on the coasts of some marine areas have reached thousands of particles per cubic meter (Osman et al., 2023).

Microplastics can also be easily swallowed by aquatic creatures due to their small sizes (Schell et al., 2021; Szymańska and Obolewski, 2020). Based on their widespread presence in the environment (from the summit of Mount Everest to the deepest oceans), MNPs are inevitably absorbed by organisms (via food, water or by breathing in), and can pose a serious risk to both animal and environmental health (Ma et al., 2023; Berkel and Özbek, 2024). Research shows that some internal organs are damaged when microplastics are accidentally swallowed by aquatic creatures (Wright et al., 2013; Issac and Kandasubramanian, 2021). A number of marine animals including sea turtles, whales, fish, dolphins, otters and seals has been reported to die by swallowing plastics found in their natural habitats or suffocating when it becomes entangled in their bodies (Umaru et al., 2019). People exposed to MNPs may experience increased risk of negative physiological effects such as oxidative stress, metabolic disorders, immune response (increased inflammation), neurotoxicity, insulin resistance and cancer (Feng et al., 2023; Yee et al., 2021; Liu et al., 2024).

The analysis of MNPs in various environmental samples is carried out using methods such as FT–IR/microFTIR, Raman/micro-Raman spectroscopy, TEM/SEM, and GC–MS (Fig. 2) (Wu et al., 2023). Each of these methods has considerable advantages in addition to their potential limitations in routine environmental analyses of MNPs. The advantages and disadvantages of these commonly used methods in the analysis of micro(nano)plastics are detailed in Fig. 3 (Beattie et al., 2022; Gaba et al., 2022; Selamat et al., 2021; N'cho et al., 2016; Dobrzyniewski et al., 2021).

In this review, we cover different methods used in the identification and quantification of MNPs, especially from water environments including seas and lakes.

2. Spectroscopic techniques

2.1. FTIR and micro–FTIR spectroscopy

FTIR spectroscopy is the most common technique used in the identification and quantification of microplastics, followed by Raman spectroscopy in terms of importance (Yakovenko et al., 2020; Chen et al., 2020). Visible MPs are generally identified by conventional FTIR, whereas the identification of smaller particles requires the use of micro–FTIR (μ–FTIR), which is equipped with microscope to localize MPs on filters. In theory, MPs with a diameter of 10 mm can be detected by micro–FTIR (Munoz et al., 2018; Harrison et al., 2012; Shim et al., 2017; Vianello et al., 2019). The μ-FTIR imaging equipped with focal plane array (FPA) detectors enables a much faster generation of chemical map of microplastics by simultaneously recording several thousand spectra within a single run (Primpke et al., 2017; Loder et al., 2015).

FTIR imaging can be used to analyze diverse samples directly on filters without any visual presorting, when the sample obtained from the environment was previously extracted, purified, and filtered. However, this spectroscopy approach is highly restricted by the limited IR transparency of conventional filter materials. To overcome this limitation of FTIR imaging, Käppler et al. developed a novel silicon (Si) filter substrate, which provides a sufficient transparency for the broad mid-infrared region of 4000–600 cm^{-1} (Käppler et al., 2015). Authors also

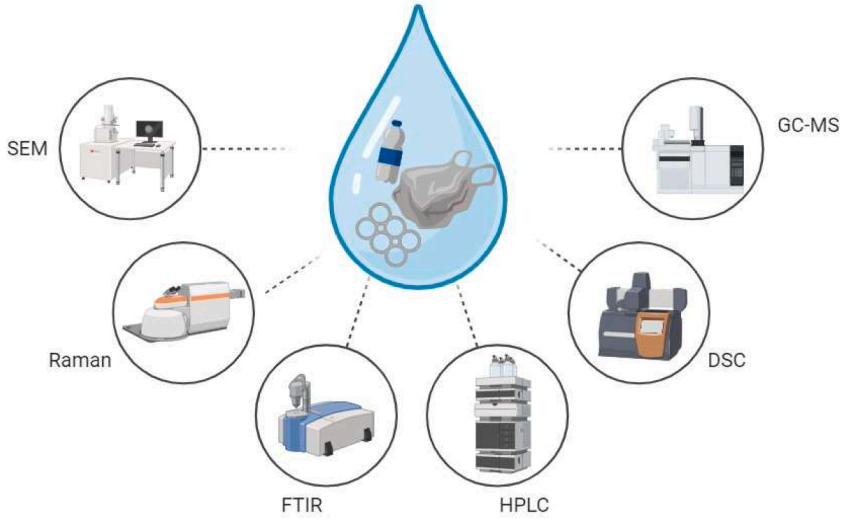

Fig. 2. Some methods used in the determination of MNPs.

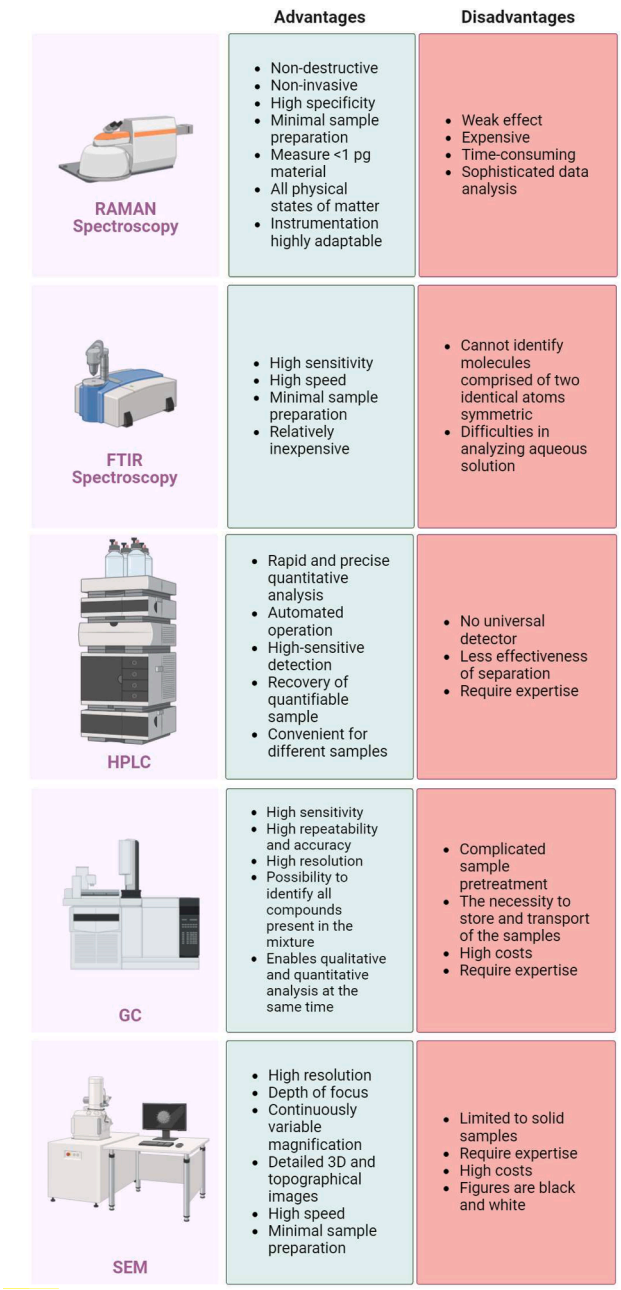

Fig. 3. Certain advantages and disadvantages of commonly used methods in the analysis of MNPs in environmental samples.

showed that this Si filter substrate makes a distinct identification of PE and PP in the characteristic fingerprint region (1400–600 cm^{-1}) possible. Using this Si filter substrate and FTIR imaging, microparticles of polyesters having quite similar chemical structures, such as PET and PBT, were shown to be differentiated, facilitating a visualization of their distribution within an environmental sample. Moreover, this Si filter can also be utilized as a substrate for Raman microscopy to identify MNPs (Käppler et al., 2015).

Rathore et al. developed, optimized, applied, and validated μ–FTIR techniques for the identification of MPs in the range of 20 μm – 1 mm, using PE, PP, PS, PA and PVC as standards (Rathore et al., 2023). Authors validated the accuracy of their results by comparing results from μ–FTIR with FTIR–ATR (Attenuated Total Reflectance), and found that the two spectra are comparable, showing the similar pattern of the polymeric composition. Their analyses also showed that the reflection mode (particularly diffuse reflection) is more efficacious in terms of the quantification of smaller-sized microplastics in complex environmental samples. Authors also successfully applied this method to a representative environmental sample (sand) (Rathore et al., 2023).

Morgado et al. reported a methodology to identify the most abundant polymer types in aquatic sediments (which are sampled from Ria de Aveiro, Ria Formosa, and Mira River (Portugal)) by micro–ATR–FTIR (Morgado et al., 2021). Their strategy to identify the polymer type of MNPs included a sequence of spectra comparisons with diverse reference spectra considering defined signal requirements and different wavenumber ranges, signal processing, match algorithms and target match values. The definition of signal requirements make it possible for them to reduce the vulnerability of their method to falsely assuming a polymer identity. Authors successfully applied this micro–ATR–FTIR method to the identification of PP, PE, PS and PET particles in aquatic sediments.

Tagg et al. developed a method based on FPA–based reflectance μ–FTIR imaging to detect MPs within complex and organic-rich wastewater samples, and applied and experimentally validated it (Tagg et al., 2015). Authors first employed a pre-treatment step using 30 % hydrogen peroxide in order to remove biogenic material/organic matter from wastewater and also to aid sample filtration. They showed that FPA–based reflectance μ–FTIR imaging can successfully image and identify 5 microplastic types: PE, PP, nylon-6, PVC and PS. Their method was nonselective and reproducible with the overall identification success rate of 98.33 %. Besides, the use of this method provided a significant reduction in analysis time when compared to other previously reported methods, since samples which could take multiple days to be mapped using a single-element detector can be imaged in shorter than 9 h (circular filter with a diameter of 47 mm) using this method.

2.2. *Raman spectroscopy*

Raman spectroscopy is a vibrational spectroscopy method which uses inelastic scattering of light, where the frequency shift identifies the roto-vibrational excitations of molecules. Based on its broad vibrational frequency range, high spatial and spectral resolution, and its operability in the visible or near-infrared range (in which many organic materials and water are transparent), Raman spectroscopy has been widely used for the detection of MNPs in various samples (Ribeiro-Claro et al., 2017). The advantage of spectroscopy techniques such as micro–FTIR and micro–Raman is that they allow the determination of the composition of individual MPs without the need to destroy the samples (Zangmeister et al., 2022).

Kniggendorf et al. presented a method for the detection of individual small microplastic particles of sizes around 0.1 mm in tap water streaming with 1 L/h, based on Raman spectroscopy (Kniggendorf et al., 2019). Their setup did not require additional sampling or sample processing steps. Authors reported that individual particles of PA, PE, PMMA, PP and PS in streaming tap water can be determined with a lowest signal-to-noise ratio of 5 using their Raman lines between 2800 and 3100 rel. cm^{-1}, even in the raw data. Wu et al. reported the development of a line scan confocal Raman μ-spectroscopy tool for the quick detection and identification of MNPs, which increases the speed of imaging by 1–2 orders of magnitude when compared to point confocal Raman imaging (Wu et al., 2024).

Gillibert et al. developed Raman Tweezers (RTs), optical tweezers combined with Raman spectroscopy, as an analytical method to study of MNPs in both distilled water and seawater samples (which are sampled from Mediterranean Sea, in Torre Faro (Messina, Italy)) (Gillibert et al., 2019). Authors reported the optical trapping and chemical identification of sub–20 μm MNPs of PP, PS, PE, PA6, PVA, PMMA and PET, down to the 50 nm range. Besides, analysis at the single particle level allowed them to clearly discriminate plastics from organic matter and mineral sediments, overcoming the potential of standard Raman spectroscopy in liquid, inherently limited to ensemble measurements. Moreover, being a microscopy technique, RTs allowed the assessment of the sizes and

shapes of MNPs (beads, fragments, and fibers), with spatial resolution only limited by diffraction.

2.2.1. Surface-enhanced Raman spectroscopy

Surface-enhanced Raman spectroscopy (SERS) is a highly sensitive technique which allows the Raman scattering of molecules supported by some nano-structured materials (Han et al., 2021). Very recently, Qi et al. used SERS methodology based on two dimensional AuNPs thin films to identify MNPs in water samples (Qi et al., 2024). In this study, the single particle detection of PS and PMMA was achieved owing to the hot spot region created by the electromagnetic amplification of 2D AuNPs thin films. Authors reported that the SERS-active substrate has a high SERS property in the single particle detection of MNPs as small as 200 nm, and has a good stability and reusable performance after 5 cycles of use. Furthermore, they found the enhancement factor to be up to 62.48.

Similarly, others used SERS sensors for the quantification of MNPs in diverse environmental water samples. Li et al. reported the development of a novel honeycomb–like AgNPs@TiO_2 array-based SERS sensor for the detection of MNPs in tap water, lake water, soil water and sea water (Bohai Sea, China), with limit of detection (LOD) values of 100 μg/mL, 100 μg/mL, 100 μg/mL, 100 μg/mL and 250 μg/mL, respectively (Li et al., 2024). The recovery rates of PS microspheres in these 4 water environments were in the range of 97.6–109.7 %, with the RSD in the range of 0.49–10.23 %, showing practical environmental analytical applicability of the developed honeycomb–like AgNPs@TiO_2 array–based SERS sensor.

3. Mass spectrometry methods

Mass spectrometry (MS) comprises a range of advanced analytical techniques which can be applied for the detection and determination of material structure and composition. Based on its advantages such as quick and reliable analysis, ease of operation, high sensitivity, high-throughput analysis, MS methods have attracted increasing attention in terms of the direct identification of polymeric structures. The basic principle of these methods is based on the ionization of the MPs followed by the separation of molecular constituents according to their m/z (mass-to-charge ratio) values. The MS analysis further characterizes the types and nature of the MPs via the determination of the repeating unit mass, end groups, and chemical formula (Wu et al., 2023; Wu et al., 2020; Lin et al., 2020). The use of MS instead of spectroscopy implies a highly different approach in terms of sample preparation and provides a distinct data; and sample preparation is critical to successful MS, particularly when analyzing complex matrices. Mass-related analysis of MNPs is complementary to the spectroscopic characterization of these particles by micro–FTIR/micro-Raman. All these methods contribute to a different understanding of MNP behavior in the environment. Besides, multi-scale characterization enables a better understanding of the complex interactions of MNPs with natural constituents and their reactivity (Schwaferts et al., 2019; Renner et al., 2019; Zhang et al., 2024). The first study on the identification of MNPs using MS was published in 2013, where authors used Pyr-GC/MS (pyrolysis–gas chromatography-MS) to analyze microplastics in the sea water near Norderney Island (Germany), which is also detailed below (Fries et al., 2013). A review on MS as a tool for MNP analysis, including the pre-treatment methods, various MS techniques, comparison between MS and other techniques have been published recently (Zhang et al., 2024).

3.1. ICP–TOF–MS

Vonderach et al. developed a downward pointing ICP (inductively coupled plasma) coupled to a time-of-flight mass spectrometer (ICP–TOF–MS), which allows quantitative transport of large micro-droplets (diameters up to 90 μm) into the ICP, for the quantitative analysis of microplastic particles (Vonderach et al., 2023). In the study, polymer microbeads were transported via monodisperse microdroplets into a downward-pointing ICP, and later analyzed by ICP–TOF–MS, allowing for multiplexed analysis at high time resolution which enables the precise identification of droplet and beads based on tracer signals, besides monitoring their carbon content and other metals present. The carbon content of single PS microbeads were successfully determined using this method. Authors stated that the accurate quantification of C in single and sufficiently large micron-sized plastics (for instance size of $\leq$ 10 μm) is possible using this method, as they showed for 3 μm–sized microbeads, therefore it could be a highly suitable approach for the analysis of microplastics in the future.

3.2. HS–SPME–GC/ITMS

Ravit et al. characterized and identified organic compounds associated with solid microplastics (persistent organic pollutants (POPs)) in urban freshwaters (northern New Jersey surface waters) using solid phase micro extraction coupled with headspace gas chromatography/ion trap mass spectrometry (in short, HS–SPME–GC/ITMS) (Ravit et al., 2017). Authors stated that patterns of identified compounds were similar to patterns obtained in the analysis using Pyr–GC/MS, showing that these 2 analytic methods (SPME–GC/MS and Pyr–GC/MS) enable clear identification of compounds associated with MP debris and characterization of the most common plastic type(s).

4. Chromatographic methods

4.1. Pyr–GC–MS

Contrary to spectroscopic methods, thermoanalytical techniques are destructive methods since the sample is thermally decomposed under certain conditions, using specialized units including pyrolyzers or thermogravimetric systems (Fabbri, 2001; Dümichen et al., 2015; David J and Kucerik J, 2018). The formed pyrolysis (a method of thermochemical conversion; the heating of an organic material in the absence of oxygen) products are then analyzed via gas chromatography coupled with MS (GC/MS). The respective type of polymer is then identified by its specific decomposition products. Thermoanalytical methods can be used either qualitatively for single MNP particles, their organic additives and rubbers, but also for the simultaneous quantification of complex environmental samples to identify MNP polymer types and their respective products, as detailed below.

Sullivan et al. used pyrolysis - gas chromatography–time of flight mass spectrometry (Pyr–GC–TOF–MS) to determine certain MNPs (PP, PS, PVC) in water samples (Sullivan et al., 2020). Authors used PTFE membranes as sample supports in their method. They determined detection levels for PVC and PS to be below <50 mg/L, with repeatable data showing good precision (RSD% of <20 %), and applied this method for the semi-quantification of MNPs in river water samples collected from River Tawe, South Wales for which the results identified several marker ions for PS, but markers for PP and PVC were not observed.

Same method was also used by others for the quantitative analysis of nanoplastics in environmental and potable waters. Okoffo and Thomas used Pyr–GC/MS for the simultaneous identification and quantification of 9 different nanoplastic types (PE, PC, PP, PS PET, PMMA, PVC, nylon 6 and nylon 66) in environmental and potable water samples (including wastewater, stormwater, reservoir water, municipal (tap) water (Queensland, Australia), surface water and bottled water) based on polymer–specific mass concentration (Okoffo and Thomas, 2024). They used a pre-treatment method which uses hydrogen peroxide digestion and Amicon® Stirred Cell ultrafiltration preconcentration together. Limits of quantification in this study were in the range of 0.01–0.44 μg/L (0.04 μg/L for PP, 0.07 μg/L for PE, 0.44 μg/L for PC, 0.05 μg/L for PS, 0.10 μg/L for PMMA, 0.04 μg/L for PET, 0.01 μg/L for Nylon 6, and 0.03 μg/L Nylon 66), and the majority of the selected nanoplastics were detected at the concentration range of 0.04–1.17 μg/L, except for PC,

which was consistently below the limit of detection (<0.44 μg/L). The prevalent polymer components in these water samples were PS (0.06–0.53 μg/L) nanoplastics, PE (0.10–1.17 μg/L), PET (0.06–0.91 μg/L) and PP (0.04–0.79 μg/L) NPs (Okoffo and Thomas, 2024).

In another study, Pyr–GC/MS was used to assess the mass concentrations of MNPs in waste water treatment plants (WWTPs), comparatively between influents and effluents (Xu et al., 2023). Using this method, authors found that the mass concentrations of total MNPs decreased from 26.23 and 11.28 μg/L in the influent to 1.75 and 0.71 μg/L in the effluent (following primary, secondary, and tertiary treatment processes), with removal rates of around 93 %, at two different plants in China. They reported that the proportions of NPs (0.01−1 μm) were 12.0 − 17.9 and 5.6 − 19.5 % in these WWTPs; and among these, PE PP and PET were the dominant polymer types in wastewater; whereas PS, PA and PMMA only accounted for a small part. The removal efficiency of NPs was also reported to be lower than that of MPs (>1 μm). Based on annual wastewater effluent discharge, they estimated that approximately 0.321 and 0.052 tons of MPs and NPs were released into the river each year. Others used Pyr-GC/MS for the qualification and quantification of synthetic microfibers (PET, nylon-6, and PAN) emitted from textiles in the course of the laundering process, by applying a sequential process which involves the filtration of laundry wastewater and solvent extraction with hexafluoroisopropanol (HFIP) (Lim et al., 2022). Authors of this study reported that the detection and quantification limits were lower than 0.2 μg and 0.6 μg for all polymers, respectively. The quantification results for the microfibers extracted from the textile made from a single filer in this study showed that PET, N-6, and PAN textile produced 481, 111, and 329 mg of MFs per kg textile, respectively. Compared to the single textile (PET), the blended textiles were shown to produce larger amounts of MPs, 961 mg kg^{-1} for PET/cotton and 680 mg kg^{-1} for PET/wool blended textiles, pointing to the easier formation of microfibers from blended textiles in the course of textile laundering. Authors also stated that TGA (thermogravimetric analysis that monitors the loss and/or gain of sample mass as a function of temperature / time) is required in the pre-analysis step prior to Py–GC/MS to obtain a suitable HFIP dilution factor due to the wide microfiber weight range from sub mg to 1000 mg per kg textile.

Hermabessiere et al. optimized and validated a Pyr–GC/MS method, and determined LOD for 8 common polymers, applied it to environmental samples such as those isolated from beach sediments, sea water surface, and bivalves collected in the marine environment, and also compared its performance with μ-Raman spectroscopy (Hermabessiere et al., 2018). In their report, the optimized Pyr-GC/MS method required a pyrolysis temperature of 700 °C, a split ratio of 5, and 300 °C as injector temperature. All LODs were found to be below 1 μg. Besides, authors showed that Py-GC/MS enables the identification of pigment containing particles just after μ-Raman analysis, and identifies co-polymers including PE–PP or PE–PP–PA6 which are hard to identify with μ-Raman without the use of chemometrics approach. Similarly, Fries et al. applied Pyr–GC/MS to simultaneously identify polymer types of marine MP particles and associated organic plastic additives (OPAs) in one run, in marine sediments collected from Norderney, a North Sea island (in Lower Saxony's Wadden Sea National Park) (Fries et al., 2013). They found that the particles identified consisted of PE, PP, PS, polyamide, chlorinated PE and chlorosulfonated PE. Furthermore, the polymers contained dibutyl phthalate, diethylhexyl phthalate, diethyl phthalate, diisobutyl phthalate, dimethyl phthalate, benzaldehyde and 2,4-di-tert-butylphenol. This method had a good degree of sensitivity in terms of the analysis of plasticisers, antioxidants and flavouring agents in MP particles with sample masses <350 mg, pointing to the risk posed by marine plastic debris, since some of the OPAs identified in this study have toxic and/or endocrine-disrupting properties.

Santos et al. applied Pyr–GC/MS for the simultaneous analysis of 12 most common plastic polymers found in environmental samples collected in three Mediterranean beaches of Girona (NE Spain) (Santos et al., 2023). Their method showed a good linearity for all the plastic polymers ($R^2 > 0.97$), and LOD between 0.1 (polyurethane) to 9.1 μg (polyethylene). The method precision (RSD%) was reported to be, in general, below 20 %. Authors selected the most suitable characteristic pyrolyzate compounds and respective indicator ions for each polymer type in order to obtain the most suitable response for analytical purposes. Besides, they used commercial pyrolyzates and polymers libraries to confirm the identity of the detected MPs.

Same methodology was used and optimized by the others for the identification and quantification of PS, PE, PP, PVC, and PMMA in the edible parts of 5 different seafood species (oysters, prawns, crabs, squid, and sardines). PVC was detected in all samples, and PE was detected at the highest total concentration of between 0.04 and 2.4 mg per gram of tissue. Authors reported that sardines contain the highest total plastic mass concentration (0.3 mg g^{-1} tissue), and squids have the lowest concentration (0.04 mg g^{-1} tissue), showing that total concentration of plastics is highly variable among different species, and that MP concentration differs even between the organisms of the same species. Authors also studied the use of an alkaline digestion procedure prior to an accelerated solvent extraction method with a solvent at high temperature and pressure in order to dissolve and extract plastics from these seafood samples, prior to Pyr–GC/MS (Ribeiro et al., 2020).

Nuelle et al. used an approach based on Pyr–GC/MS to identify microplastics in marine sediments collected from the North Sea island of Norderney (Nuelle et al., 2014). First, they developed a 2-step method to extract MPs from sediments: pre-extraction using the air-induced overflow method, based on fluidisation in a saturated NaCl solution, and the subsequent flotation step of microplastics with high–density sodium iodide (NaI) solution. Authors reported that recoveries of the whole procedure for PE, PP, PVC, PET, PS and PU with sizes of around 1 mm are between 91 and 99 %. They stored these samples in a 35 % H_2O_2 solution for one week, and later found that 92 % of selected biogenic material dissolved completely or had lost its color, while the tested polymers were more resistant to this effect by H_2O_2 solution. In another study, Ravit et al. used Pyr–GC/MS to determine microplastics in urban New Jersey freshwaters (heavily urbanized Raritan and Passaic Rivers), and identified three types of plastic polymers (Ravit et al., 2017).

Tan et al. used this method to study microplastic and associated polycyclic aromatic hydrocarbon (PAH) contamination in the surface water from the Feilaixia Reservoir of Beijiang River, Guangdong Province, China (Tan et al., 2019). Authors reported that the average abundance of microplastics was 0.56 ± 0.45 items per cubic meter. Six kinds of polymers, including PE, PP, PS, expanded PS (EPS), PVC and PET were detected in this river, among which PP (52.31 %) and PE (27.39 %) had the highest concentrations. Four different shapes of microplastics (namely, foams, films, fibers and fragments) were found to be present in surface water samples in this study, and among which films (37.78 %) were the most frequent shape of MPs. The most common typical size of the plastic particles was reported to range from 0.6 to 2 mm (41.36 %). The total concentration of the 16 PAHs carried on the EPS, PE and PP microplastics was reported to range from 282.4 to 427.3 ng/g; chrysene, benzo[ghi]perylene, and phenanthrene were abundant in the surface water samples obtained in this study, at concentrations of 39.5–89.6 ng/g, 34.6–56.8 ng/g and 25.6–45.6 ng/g, respectively. Considering the ratios of the PAH isomers (Flut/Py < 1 and Phe/Ant >10), the authors of the study suggested that these PAHs may be originated from the imperfect combustion of fossil fuels.

Primpke et al. performed a comparison of Pyr–GC/MS and hyperspectral FTIR imaging spectroscopy methods for the analysis of microplastics, or in general a comparison between a spectroscopy and a thermoanalytical method, on exactly the same samples (surface water, sediment and treated waste water samples) (Primpke et al., 2020). They reported that while the overall trends in MP contamination were found to be very similar when these two different methods were used, differences were observed in the polymer compositions. Authors stated that while hyperspectral FTIR imaging spectroscopy detected a wide range and even highly low numbers of smaller-sized particles; Pyr–GC/MS,

when exceeding a certain detection threshold, allowed a condensed overview of different polymer types represented by a shared chemical backbone expressed by basic polymer clusters.

Ishimura et al. studied the effect of the use of calcium carbonate ($CaCO_3$) as a catalyst on pyrolytic behavior of multiple polymers to obtain catalytic conversion of reactive pyrolyzates to more stable compounds amenable to GC/MS analysis (Ishimura et al., 2021). $CaCO_3$ was also used as a diluent for insoluble PP and PE powders to ensure weighing easiness by forming a homogenous mixture. In this study, firstly, they prepared a reference material to make calibration curves by mixing 12 types of standard polymers. The identification and quantification of polymers in these mixed samples of polymer were validated by using model polymer mixtures, following the storage of Py-GC/MS data of 12 polymers with a given sample amount in F–Search MPs software. Results exceeding the LOQ combined with the high probability of a library match as confirmed by the software, confirmed the presence of the identified polymer in the model polymer mixtures. The marine and beach samples were successfully analyzed for the identification and quantification of MPs by this Pyr–GC/MS method in the presence of $CaCO_3$ in this study.

Vilakati et al. used Pyr–GC–TOF–MS to analyze and characterize microplastics in a wastewater treatment plant (WWTP) in Gauteng Province of South Africa (Vilakati et al., 2021). Authors found that there are 23 pyrolyzate products with contributions from PVC, PA, PET and PE with abundances of 47.8 %, 13.1 %, 17.4 % and 4.3 %, respectively; and stated that the remaining portion (17.4 %) could be attributed as additive compounds in MPs. The fragmented pyrolyzate products from MPs were found to belong to the family of polyaromatic hydrocarbons, monoaromatic hydrocarbons, acyclic alkanes and fatty acids. Besides, additives including isopropyl palmitate, DEHP, 2-ethylhexadecyl ester of hexanoic acid and undecanoic acid were detected by the authors in the extracted MPs from the samples obtained from the WWTP. The thermal studies in this paper confirmed the presence of aluminum, calcium and silicon as residues of catalysts or flame retardants or UV stabilizers in MPs or as adsorbates resulting from the surface adsorption from the surroundings. The WWTPs methodology used in this study confirmed the identity of the diverse fragments related to the MPs monomers. Similarly, Lin et al. reported a method for the determination and quantification of MNPs based on thermal fragmentation and MALDI–TOF–MS (matrix-assisted laser desorption/ionization time-of-flight mass spectrometry) using PS particles as a model MNP (Lin et al., 2020). Using this method, the PS MNPs were identified by fingerprint peaks in both low-mass (m/z values of 90, 104, 128, 130, and 312–318) and high–mass regions (repeated peaks with $\Delta m/z$ 104 in the m/z range of 350–5000), and the quantification of PS MNPs was carried out with m/z of 315.3. In this study, the different ionization behaviors allowed the differentiation of MNPs with distinct molecular weights. Authors also found that a simple thermal pretreatment at 380 °C can enable the fragmentation of PS, resulting in the significant enhancement of the intensities of fingerprint peaks in low-mass regions, ultimately allowing a detection limit of 25 ng for PS MNPs. The applicability of this method based on MALDI–TOF–MS in different sample matrices (such as fish samples from a local market (Beijing, China) and water samples collected from a river in the Olympic Park region of Beijing) and for other types of MNPs such as PET (to show the universality of the method) was also successfully shown by the authors in this study.

Similarly, Castelvetro et al. also used Py–GC/MS method for the accurate and selective determination of the polymers most frequently found as MPs polluting marine and freshwater sediments (Castelvetro et al., 2021). Authors also described a multi-step fractionation and purification protocol and multi-analytical approach, allowing the accurate polymer-specific detection and quantification of the total mass content of contaminating MPs and NPs in marine and lakebed coastal sediments.

4.2. TED–GC–MS

The thermal extraction desorption gas chromatography-mass spectrometry (TED–GC–MS) analysis is a 2-step method in which a sample is initially decomposed in a thermogravimetric analyzer (TGA), and the resulting gaseous decomposition products are then trapped on a solid-phase adsorber. Later, this solid-phase adsorber is analyzed using thermal desorption gas chromatography mass spectrometry (Dümichen et al., 2019).

Funck et al. used this method to compare the influence of continuously and discontinuously backwashed sand filters to retain MPs from secondary treated wastewater effluents from three full-scale WWTPs (Funck et al., 2021). Authors targeted four common polymers (PP, PE, PS, and PET), and found that PE was the most frequently found polymer detected in secondary effluents, with normalized annual loads in the range of 2.8 mg $yr^{-1}P.E.^{-1}$–8.4 mg $yr^{-1}P.E.^{-1}$. Their data showed that sand filters offer additional efficient microplastic retention capabilities, providing, on average, an extra 79 % ± 11 % of MP retention when compared to secondary treatment. Authors stated that the high-volume sampling system in combination with the non-discriminatory mass--based analysis method using an automatized TED–GC–MS technique enables a rough classification of MP sizes, and estimating the annual mass emissions of MPs in the secondary and tertiary treated effluents in a statistically robust manner.

4.3. LC–UV

Müller et al. used liquid chromatography with UV detection (LC–UV) for the analysis of PET MP particles following alkaline extraction of PET from the environmental matrix samples including sewage sludge and suspended particles from urban water management systems (Müller et al., 2020). Using this method, they subsequently determined the monomers of PET, terephthalic acid. In this study, recoveries for model samples were reported to be between 94.5 % and 107.1 %; and LOD and LOQ were calculated to be absolute masses of 0.031 and 0.121 mg PET, respectively. Authors also verified the measured mass contents of microplastic particles in these environmental samples, by performing a method comparison with thermal extraction-desorption-gas chromatography–mass spectrometry (TED–GC/MS), and found that both methods deliver comparable results and corroborated each other.

A 3-step method for the quantification of the mass of PET MNPs in complex environmental matrices was developed by Tian et al. based on a simplified in-matrix depolymerization (using ethylene glycol) combined with LC–UV (Tian et al., 2022). The limit of quantification (LOQ) for PET was found to be 0.2 μg/g for wet sewage sludge sample (obtained from the Waternet water treatment plant in Horstermeer of the Netherlands), and the concentration of PET MNPs in liquid sewage sludge was measured as 1.5 mg/L.

4.4. *Reversed–phase HPLC*

Castelvetro et al. reported an analytical procedure to quantify the total mass of PET MNPs in sediments, which involves aqueous alkaline PET depolymerization with phase transfer catalysis, oxidation and fractionations (purification) to remove interfering species (for instance, most biogenic materials that are generally present in lake and seabed sediments) and pre-concentrate the terephthalic acid (TPA) monomer, and ultimately quantification of TPA by reversed–phase HPLC (Castelvetro et al., 2020). Authors found that TPA recovery from a model sediment spiked with 800 ppm PET micropowder was 98.2 %, with LOD as 17.2 μg/kg and LOQ as 57.0 μg/kg. Analyses of sandy sediments from a marine beach on the northern coast of Tuscany (Italy) by this method showed that MNP contamination is in the 370–460 μg/kg range, proving that a significant fraction of PET microfibers released in surface waters ends up in shore sediments. Furthermore, authors stated that the presence of 300–500 ppb PET, a comparatively high amount in a

beach sediment for a polymer particle with density much larger than marine waters, can be primarily ascribed to microfibers transported via current and waves, with potentially a small contribution from airborne contamination.

5. Thermal analysis in general and other thermoanalytic methods

In one study, sedimented freshwater suspended organic matter fortified with PP, PE, PS, and PET particles was used in an inter-laboratory comparison of thermoanalysis methods for MNP identification and quantification (Becker et al., 2020). Three laboratories carried out analysis using Py–GC–MS, three others used TED–GC–MS. One laboratory conducted thermogravimetry–infrared spectroscopy, and 2 participants used thermogravimetry coupled to mass spectrometry. Other laboratories used differential scanning microscopy (DSC), a procedure based on micro combustion calorimetry (MCC) and a procedure based on elemental analysis. Each participating laboratory used a distinct combination of sample treatment, calibration and instrumental settings. Although it was reported that there is still room for improvements in terms of the between-laboratory reproducibility and the harmonization of procedures, it was observed in this study that the participants performing Py–GC–MS, TED–GC–MS, and TGA–FTIR were able to accurately identify all polymers and to report rational quantification results in the studied concentration range. Although there are certain limitations in terms of the detection of specific polymers for the other methods, they showed potential as alternative methods. Below, we cover studies reporting the use of thermal analysis for MNP identification and quantification from diverse water samples.

5.1. *TGA–FTIR–GC/MS*

Liu et al. described a method to detect, identify, and quantify MPs present in marine mussels (*Mytilus edulis;* blue mussel) using TGA–FTIR–GC/MS method, following the extraction and isolation of the MPs using chemical digestion, density separation, and filtration (Liu et al., 2021). In their study, the combination of these 3 instrumental methods added increased discriminatory power as temperature profiles, chromatograms, and vibrational and mass spectra show differences among common plastics. This method recorded the loss in sample mass with temperature, and the associated infrared (FTIR) and mass (GC/MS) spectra of the gaseous products coming out following pyrolysis. Authors focused on four types of plastics (PP, PE, PVC and PS), and showed that TGA–FTIR–GC/MS can be optimized to easily determine both the type (polymer) and amount (mass) of MPs present in the sample. When applied to a hundred mussels from each of six different locations along the coast of China (purchased from local seafood markets in Dalian, Yantai, Lianyungang, Zhoushan, Xiamen and Shipu), authors found an average of 0.58 mg kg^{-1} of plastic per tissues, with PE being the most frequently found plastic type. Among these 6 coastal cities studied, mussels from Dalian were found to have the highest MP content, using this method.

Nel et al. used TGA–FTIR–GC–MS since this method offers a novel characterization platform that provides information on both physical and chemical properties of the analyzed polymers (Nel et al., 2021). Authors used a library of eleven polymers produced from virgin plastics and post-consumer products. In this study, TGA inflection points and mass of remaining residues after pyrolysis, in certain cases, were shown to be informative of the polymer type. FTIR analysis of the evolved gas was shown to able to differentiate between all polymers but PE and PP. Finally, they showed that GC–MS is able to differentiate between the specific chemical fingerprints of all polymers (with the exception of one polymer) in the library. Later, they used this library to characterize real environmental samples of plastic particles with sizes <5 mm sampled from beaches in the UK and South Africa, where clear identification of the polymer types was attained, with PE being the most frequently found polymer in samples collected from Kommetjie, Muizenberg and Fish Hoek (South Africa), indicating variations that possibly resulted from aging and weathering processes. Authors found that, Kommetjie, situated on the Atlantic Seaboard, has the lowest plastic contamination documented in both May and June/July, with plastic particles only observed at the end of the beach zone.

5.2. *TGA–DSC*

TGA–DSC was used to determine characteristic endothermic phase transition temperatures of 7 MP polymer types in extracts obtained from wastewater effluent samples, in a single instrument run (Majewsky et al., 2016). In other words, this technique allowed both qualitative and quantitative analysis of MP types in a sample by their differential melting characteristics. Authors reported that among the polymers studied, only PP and PE could be clearly identified, whereas the phase transition signals of the other polymers in TGA–DSC analysis largely overlap with each other. 81 mg and 257 mg PE per cubic meter were found in two wastewater samples using this method.

6. SEM

6.1. *SEM–EDS*

Miserli et al. used SEM in tandem with Energy Dispersive X–ray spectroscopy (EDS) to detect and identify microplastics in seawater and also in fish species (sea basses (*Dicentrarchus labrax)* and sea breams *(Sparus aurata*)) and mussels (*Mytilus galloprovincialis*) from aquaculture systems (in Northwest Ionian Sea), since these aquatic organisms are commonly commercially available for human consumption (Miserli et al., 2023). For biological samples, authors used a digestion step with Fenton's reagent in order to remove organic material, later followed by a filtration and a density separation step where the sample material was mixed with a saturated $ZnCl_2$ solution to isolate MP particles from heavier material. For seawater samples (sampled by a MP net sampler), they only applied sieving on stainless steel sieves prior to filtration on silica filters. With the combined use of SEM and EDS, authors were able to analyze and characterize surface morphology and elemental composition of selected MPs, and also to distinguish them. They were also able to observe weathering and fragmentation processes in SEM images, while oxidation and adsorption of metallic ions could be further confirmed by authors using EDS analysis. Others also used SEM analysis combined with EDS mapping to study the material composition of MPs in samples collected from the wastewater treatment plants (located in the Kalasalingam University campus, India) (Yuvedha et al., 2019). This methodology was even used for the identification and morphological characterization of MP fibres released from COVID–19 test swabs and also of additives such as titanium oxide particles present on the surface of these fibres (Fang et al., 2023). Similarly, Fries et al. used SEM equipped with an energy-dispersive X-ray microanalyser to identify the inorganic plastic additives (IPAs) contained in marine MP particles (Fries et al., 2013). IPAs identified in this study were titanium dioxide nanoparticles (TiO_2–NPs), barium, zinc and sulphur; therefore, authors stated that marine MPs may act as a TiO_2–NP source.

Furfaro et al. performed SEM/EDX analyses to characterize the plastic debris in the stomach content of *Bursatella leachii*, an aplysiid heterobranch (a type of benthic sea slug) living in the Mar Piccolo, a polluted coastal basin close to Taranto, in the northern Ionian Sea (in Mediterranean Sea), and found that MPs were present in the stomachs of all the specimens sampled (Furfaro et al., 2022). The SEM images and EDX spectra from this study can be regarded as a baseline reference database for further investigations in the future on marine Heterobranchia and their interactions with MNPs. Others used this method to investigate the primary sources of MPs from cosmetics available in Poland, and also to more provide more detailed description of these particles such as particle surface morphology (Dąbrowska et al., 2022).

Table 1
Certain variables/parameters of the MNPs analysis methods covered in the present review.

Method(s)	Amount of sample needed (if reported) / other amount values reported	The origin of samples (locations and other details)	The type of MNPs studied/found	Time required / other experimental time values reported	Ref
Novel silicon (Si) filter substrate for FTIR imaging, Raman microscopy		thin melt films (15 μm) of commercial pellets of HDPE, PP, PET and PBT with a heated press (Specac).	PE, PP, PET and PBT	500 ms	(Käppler et al., 2015)
μ–FTIR		environmenal samples (sand) (Western Scheldt near Yerseke, the Netherlands)	PE, PET		(Rathore et al., 2023)
μ–ATR–FTIR	50 g or 100 g of the dried sediment	aquatic sediments (Ria de Aveiro, Ria Formosa, and Mira river (Portugal))	PE, PP, PET, and PS	72 h of the digestion period	(Morgado et al., 2021)
FPA–Based Reflectance μ–FT–IR Imaging	dry plastics	wastewater samples (Severn Trent Water treatment facility, Derby, UK)	PE, PE, nylon-6, PVC, PS	pellets immersed in H_2O_2 stored for 3, 5, or 7 days; samples can be imaged in shorter than 9 h	(Tagg et al., 2015)
Raman Spectroscopy	0.5 g of microplastic and the respective contaminant in 1 L of tap water	streaming tap water (Hannover, Germany)	PA, PE, PMMA, PP and PS	sample suspensions stored in glass stoppered glass flasks at RT for 24 h before use; an average effective excitation time of 33 ms	(Kniggendorf et al., 2019)
Line scan Raman micro-spectroscopy	2 μL MNP beads suspensed in water/ ethanol solution	microplastic powders in ethanol	PS, PMMA, PA, PP, PVC	increased speed of imaging by 1–2 orders of magnitude when compared to point confocal Raman imaging; imaging a 40 μm × 10 μm area in 10 s (single step exposure time 0.5 s)	(Wu et al., 2024)
Raman Tweezers	10 μL of particles solution	seawater, distilled water, marine sediment samples (Mediterranean Sea, Torre Faro, Messina, Italy)	PE, PP, PA6, nylon, PS, PVC, PET, PVA, and PMMA	fast analysis (few seconds to few tens of seconds per spectrum) is achieved exciting in at 633 nm with powers of 11 mW. NIR lasers (785 nm) require longer analysis times (10 to 100 times).	(Gillibert et al., 2019)
SERS sensor with two-dimensional AuNPs thin films		deionized water	PS and PMMA	exposure time of 1 s; samples generated in the laboratory collected 10 times for 10 s	(Qi et al., 2024)
Honeycomb-like AgNPs@TiO_2 array SERS sensor	prior to Raman measurements, 15 μL of PS dispersion injected onto the Ag@TiO_2 nanocages substrate	environmental water samples (tap water, lake water, soil water and seawater samples (Bohai Sea, China))	PS, PMMA, PE and PP		(Li et al., 2024)
Pyr–GC/MS and SEM	each sediment sample in aliquots of 175 g	sediment and seawater samples collected from Norderney, a North Sea island (Germany)	PE, PP, PS, PA, chlorinated PE and chlorosulfonated PE	pre-conditioning at 40 °C for 60 min; temperature programme for thermal desorption from 40 to 350 °C, held for 10 min, at 10 °C min^{-1}. Cold injection system: heating to 280 °C at a heating rate of 12 °C min^{-1} and maintained at 280 °C for 3 min. The same particle pyrolysed at 700 °C for 60 s. Prior to pyrolysis, the TD temperature set to 60 °C, held for 1 min, and heated up to	(Fries et al., 2013)

(*continued on next page*)

Table 1 (*continued*)

Method(s)	Amount of sample needed (if reported) / other amount values reported	The origin of samples (locations and other details)	The type of MNPs studied/found	Time required / other experimental time values reported	Ref
				350 °C at 180 °C min^{-1}.	
Total consumption microdroplet ICP–TOFMS	4 mL / 0.1 mL of cell suspension (approximately 5 × 10^5 cells) in 1.5 mL eppendorf tube; microplastic beads (PS) and spleenocyte cells are also embedded in microdroplets	microdroplets	PS	Time-resolved droplet signals acquired continuously for 2 min per run by recording the mass spectra at a spectral averaging rate of 333 Hz (3 ms average time)	(Vonderach et al., 2023)
Pyr–GC/MS, HS–SPME–GC/ITMS	a very small piece of microplastic sample <1 mg in size	urban freshwaters (Raritan and Passaic Rivers, New Jersey, USA)	PE, PP, and PVA	For HS-SPME: extraction time of 30 min. At 55 °C (water samples) or 75 °C (solid plastics), followed by pre-incubation time of 2.58 min, agitation speed of 350 rpm, agitation for 5 s, agitation off for 2 s, SPME fiber vial penetration of 25.0 mm, desorption time of 10 min. Pyr-GC/MS: Helium carrier gas flow constantly maintained at 0.9 mL/min. Analyte elution from the GC column occurred using a temperature program that ranged from 35 °C to 320 °C over 40 min; retention times of 11.6 min or 14.57 min	(Ravit et al., 2017)
Pyr–GCTOF	For membrane samples containing only one of the plastics, 1 g of ground of the material added to 500 ml of deionised water; for mixed samples of each plastic, 0.25 g of each ground plastic used	river water samples collected from River Tawe, South Wales	PP, PS, PVC	heating from 30 °C to 500 °C at a rate of 20 °C/ms with a hold at 500 °C for 20 s; the column flow established at 1.2 mL min (ultra-pure helium) and GC oven ramp of 40–300 °C at 10 °C/min	(Sullivan et al., 2020)
Pyr–GC/MS	final collected and transferred retentate volume of 10 ± 2 mL	environmental and potable water samples including wastewater stormwater, reservoir water, municipal (tap) water samples (Queensland, Australia), surface water and bottled water samples	PE, PC, PP, PS PET, PMMA, PVC, nylon 6 and nylon 66	The first pyrolysis shot (from 100 °C to 300 °C) and the second pyrolysis shot (at 650 °C for 0.20 min (12 s)); oven temperature program: 40 °C (held for 2 min) to 320 °C at 20 °C/min (held for 14 min)	(Okoffo and Thomas, 2024)
Pyr–GC/MS	80 μL in pyrolysis cup; for calibration curve: 0.1–10 μg for PMMA, PA, and PS and 0.1–200 μg for PP, PE, and PET	samples from waste water treatment plants (WWTPs) (China)	PMMA, PP, PS, PE, PET, PA	pyrolysis temperature in single-shot mode set at 650 °C for 0.2 min,	(Xu et al., 2023)
Pyr–GC/MS	1, 10, 30, 50, and 70 μg of each PET, N-6, and PAN; 70 μL of each sample solution added to the sample cup	wastewater emitted from textile laundry	PET, nylon-6, and PAN	heating the GC oven from 40 °C (2 min hold) to 280 °C (20 min hold) at 20 °C/min with 1 mL/min of helium carrier.	(Lim et al., 2022)
Pyr–GC/MS	The size of analysis cup (AS-1020E autosampler of an EGA/PY-3030D device)	environmental samples such as those isolated from beach sediments, sea water surface, and	PE-PP, PE-PP- PA6, PE, PMMA, PS, PA-6, PET, PP, PC, uPVC	Samples are pyrolyzed at 600 °C for 1 min; initial oven program: 40 °C for 2 min, then	(Hermabessiere et al., 2018)

(*continued on next page*)

Table 1 (*continued*)

Method(s)	Amount of sample needed (if reported) / other amount values reported	The origin of samples (locations and other details)	The type of MNPs studied/found	Time required / other experimental time values reported	Ref
		bivalves collected in the marine environment		increase to 320 °C at 20 °C/min, maintained for 14 min. Other programs: 40 °C for 2 min, then increase to 200 °C at 15 °C/min followed by a second increase to 300 °C at 10 °C/min maintained for 2 min / 40 °C for 2 min, then increase to 261 °C at 13 °C/min followed by a second increase to 300 °C at 6 °C/min maintained for 2 min	
Pyr–GC/MS	aliquots of the collected samples (0.25 mg) weighted to the pyrolysis cups	environmental samples (collected in Mediterranean beaches of the province of Girona (NE Spain))	PS, PE, PP, PVC, PET, PC, PUR, Nylon 6 (N-6), Nylon 66 (N-66), PMMA, styrene-butadiene copolymer (SBR), and acrylonitrile butadiene styrene copolymer	the pyrolysis furnace temperature set at 600 °C with a pyrolysis holding time of 0.2 min; The GC oven program: 2 min at 40 °C, then increasing by 20 °C/min up to 320 °C and held for 16 min	(Santos et al., 2023)
Pyr–GC/MS	oysters: 8–17 g of wet weight per sample; prawns: 3–6 g of wet weight per sample; crabs: 45–85 g of wet weight per sample; squids: 4–7 g of wet weight per sample; sardines: 4–9 g of wet weight per sample; 80 μL of each sample directly injected into sample cups	high-commercial-value seafood species	PS, PMMA, PVC, PE, PET, PP	Sample digestion: 24 h at 60 °C; pyrolysis in single-shot mode at 650 °C for 0.2 min (12 s)	(Ribeiro et al., 2020)
Pyr–GC/MS	ten samples of 1 kg aquarium sand spiked with seven types of plastic particles	marine sediments collected from the North Sea island of Norderney	PE, PP, PVC, PET, PS, EPS and PUR	pyrolysis at 700 °C for 60 s; oven program: 40 to 180 °C at 15 °C/min and then to 300 °C at 5 °C/min, held for 12 min	(Nuelle et al., 2014)
μ–FTIR; GC–MS	1 μL samples injected into the autosampler in per injection	surface water samples from the Feilaixia Reservoir of Beijiang River, Guangdong Province, China	PE, PP, PS, expanded PS (EPS), PVC and PET and associated PAHs (polycyclic aromatic hydrocarbons)	80 °C for 2 min, then, raised to 200 °C at a rate of 20 °C/min for 2 min, then raised again to 240 °C at a rate of 5 °C/min, and finally, the temperature was raised to 290 °C at a rate of 2 °C/min	(Tan et al., 2019)
hyperspectral FTIR imaging; Pyr–GC/MS	0.5 to 50 μg weighed directly into the pyrolysis cups	surface water, marine sediment and treated waste water samples (in the regions of Oldenburg and Holdorf in Germany)	PE, PP, PS, PET, PVC, PMMA, PC, PA6 and methylendiphenylisocyanatepolyurethane (MDI-PUR)	pyrolysis time of 1 min, flow rate of 0.8 ml/min; temperature program: 35 °C (2 min) → 310 °C (30 min) at 3 °C/min; scan rate of scan rate 2.48 scans/s	(Primpke et al., 2020)
Pyr–GC/MS	80 mg PE, 20 mg PP; PVC (50.0 mg) , MDI-PU (12.5 mg), PS (10.0 mg), ABS (20.0 mg), SBR (20.0 mg), PMMA (10.0 mg), PC (5.0 mg), PET (20.0 mg), N6 (6.25 mg), N66 (22.5 mg)	marine samples (North Pacific Ocean) and beach samples (Kamilo Point (Island of Hawaii, Hawaii, USA)	PP, PE, PS, ABS, SBR, PMMA, PC, PVC, MDI-PU, PET, N6, N66,	backflushing start time of 13 min after sample loading; column oven temperature: 40 °C (2 min hold), 280 °C (20 °C min^{-1}, 16 min hold); scan speed of 4 scans s^{-1}	(Ishimura et al., 2021)
Pyr–GC–TOF–MS	about 1 mg of the sample	Samples form wastewater treatment plant (Gauteng Province, South Africa)	PVC, PA, PET and PE	thermal desorption: 40° to 300 °C (at the heating rate of 10 °C min^{-1}) and held for 10 min. pyrolysis: 700 °C for 60 s. GC oven program: 40	(Vilakati et al., 2021)

(*continued on next page*)

Table 1 (*continued*)

Method(s)	Amount of sample needed (if reported) / other amount values reported	The origin of samples (locations and other details)	The type of MNPs studied/found	Time required / other experimental time values reported	Ref
				(1 min hold) to 180 °C at the rate of 15 °C min^{-1} and then to 300 °C at the rate of 5 °C min^{-1} and held for 12 min.	
Py–GC/MS	50–100 μg	sediment samples (Lake Bracciano, Italy); marine sediment samples from a sandy beach (northern Tuscany, Italy)	PP, LDPE, HDPE, PS, and PET		(Castelvetro et al., 2021)
TGA–GC–MS.	150 μl crucibles	environmental samples; suspended particulate matter (SPM) samples (Danube river at Ulm, Germany)	PP, PE	Fast analysis within 2–3 h; thermal desorption with a temperature program of 50 to 200 °C at a heating rate of 40 °C min^{-1} and hold condition at 200 °C for 5 min	(Dümichen et al., 2019)
TED–GC–MS		WWTPs (Germany)	PE, PS, PP, and PET	each sample weighted by the TGA and heated from 25 °C to 600 °C, with a heating rate of 10 °C min^{-1} and nitrogen purge gas flow at 50 mL min^{-1}. GC temperature program: 40–300C at a rate of 5 °C min^{-1}, 4 min isothermal at 300 °C	(Funck et al., 2021)
LC–UV; TED–GC/MS	LC-UV: injection volume of 50 μl. TED-GC/MS: sample masses of 20 mg (composts, fermentation residue), variable masses between 6 and 15 mg for samples from water and air (samples from WWTP, dust)	soil, sediment, compost samples, fermentation residues, sewage sludge, suspended particles from urban water management systems, and indoor dust	PET	LC-UV: 95 % A at 0 min, 80 % A at 7 min, 80 % A at 15 min, 95 % A at 20 min and 95 % A at 30 min	(Müller et al., 2020)
LC–UV; LC–ESI–MS	injection volume of 5 μL	wet sewage sludge samples (Waternet water treatment plant in Horstermeer of the Netherlands), sand, indoor dust	PET	The mobile phase: (flow rate: 0.5 mL/min) The percentage of organic mobile phase B increased linearly and the gradients are as follows: 10 % at 0 min, 90 % at 15 min, 100 % at 18 min, and maintained at 100 % during 18–19 min; at 22 min, the eluent restored to the initial conditions for 1 min to re-equilibrate the column for the next injection	(Tian et al., 2022)
RP–HPLC	1 mL of hydrolyzate; mixture injected in a 50 μL loop of the instrument.	Marine samples (Tuscany, Italy), freshwater sediment samples	PET	reaction time (h) of 2–4; 0.8 mL/min flow rate;	(Castelvetro et al., 2020)
Pyr–GC–MS, TED–GC–MS, and TGA–FTIR	1 g of the spiked sediment, 0.5 g of the untreated sediment; sample intake of 1.2–0.1.3 mg, 20 mg, 0.5 mg (Py-GC–MS), 15 mg, 10–11 mg, 15–16 mg (TED-GC–MS), 20 mg (TGA-FTIR), 6 – 20 mg	Sedimented freshwater suspended organic matter	PP, PE, PS, and PET	Varied depending on method	(Becker et al., 2020)

(*continued on next page*)

Table 1 (*continued*)

Method(s)	Amount of sample needed (if reported) / other amount values reported	The origin of samples (locations and other details)	The type of MNPs studied/found	Time required / other experimental time values reported	Ref
	(TGA-MS), 25 mg (TGA-MS)				
TGA–FTIR–GC/MS	200 μg of each type of microplastics (PE, PP, PS, PVC) mixed into 2 g samples of mussel homogenate	mussels from coastal China (Dalian, Yantai, Lianyungang, Zhoushan, Xiamen and Shipu)	PE, PS, PP, PVC	the crucibles heated from 30 to 650 °C, at a ramp rate of 30 °C min^{-1} from 30 to 300 °C and 15 °C min^{-1} from 300 to 650 °C, all in a nitrogen atmosphere with a purge rate of 30 ml min^{-1}	(Liu et al., 2021)
TGA–FTIR–GC–MS	Plastic samples loaded into sample crucibles circa 6.6 mm in diameter and 1.95 mm in height, for pyrolytic decomposition	environmental samples from beaches in the UK and South Africa (Kommetjie, Muizenberg and Fish Hoek)	PE, PP, PS, EPS, PET, PA-6, uPVC, pPVC, PC, PMMA, PTFE, PU, and PLA	TGA: 50 °C for 1 min then increased from 50 to 280 °C at 120 °C/min followed by a 12.5 °C/min increase to 700 °C; additional purging step: from 700 to 950 °C at 500 °C/min, at which point the gas flow was switched to an oxygen flow of 60 mL/min for 15 min FTIR: at 280 °C with a run time of 60 min GC–MS: 40 °C - 300 °C, which was increased at 10 °C/min, maintained at 300 C for 5 min; Mass spectral data collected from 45 to 250 *m/z* for 31 min with a scan time of 0.25 s and an interscan delay of 0.05 s	(Nel et al., 2021)
TGA–DSC	Cubicle volume of 85 μL	wastewater effluent samples of a municipal WWTP (Neureut wastewater treatment plant in Karlsruhe, Germany)	PA, PES, PET, PU, PE, PVC, PP	heating from 20 to 800 °C with 5Kmin^{-1}; the total instrumental runtime of 2.7 h	(Majewsky et al., 2016)
Combined use of FTIR, SEM–EDS and μ–Raman Spectroscopies	–	samples from aquaculture systems (Fishes (*Dicentrarchus labrax, Sparus aurata* (Northern Ionian Sea)), Mussel (*Mytilus galloprovincialis*) (Thesprotia,Epirus, Greece), and water samples (seawater, near Igoumenitsa, Northwestern Ionian Sea))	PE, PP, PS, PET, PVC, PTFE, LDPE, PVB, PBMA, EVA, PVA, EAA, Nylon, PEO	Micro-Raman Analysis: The integration time is 20–200 s (usually 200 s), and the cumulation number is 1–10 times (usually 5	(Miserli et al., 2023)
SEM–EDS		Samples from wastewater treatment plants (located in the Kalasalingam University campus, southern Tamil Nadu, India)	PS, PP, PET, PVC, PELD, PEHD		(Yuvedha et al., 2019)
SEM–EDS		COVID-19 test swabs	PS, PET, PE, PVC, PP, PA, PA-6, PMMA, PC, PUR, ABS, rubber, PTFE	2–15 s of mimicked sampling	(C. Fang et al., 2023)
SEM/EDX		stomach content of *Bursatella leachii*, an aplysiid heterobranch (a type of benthic sea slug) living in the Mar Piccolo, coastal basin close to Taranto, in the northern Ionian Sea (in Mediterranean Sea)	PP, PE		(Furfaro et al., 2022)
Raman spectroscopy; SEM/EDS	micro spatula (~150 mg) of the cosmetic sample	cosmetics available on the Polish market	PE, PP		(Dąbrowska et al., 2022)

(*continued on next page*)

Table 1 (*continued*)

Method(s)	Amount of sample needed (if reported) / other amount values reported	The origin of samples (locations and other details)	The type of MNPs studied/found	Time required / other experimental time values reported	Ref
	dissolved in 10 mL of ultrapure water	(including scrubs, peelings, toothpaste, cleaners, shower gels, shampoo etc.)			
SEM–EDS	samples prepared by placing individual pieces > 0.7 mm on double-sided adhesive carbon discs (9 mm diameter), mounted on 9 mm specimen stubs	sediment of a freshwater urban river in Scotland, UK (River Kelvin located in the west end of Glasgow)	PE, PP, PS, Nylon	–	(Blair et al., 2019)
SEM–EDS		regurgitated pellets of the common kingfisher (Alcedo atthis) sampled along the Ticino River (North Italy)	PET, PU, PP, PE, PVC		(Winkler et al., 2020)
SEM–SERS	The muscle tissue of bighead carp (*Aristichthys nobilis*) dissected between the pectoral fin and vent of the fish, then minced into small pieces and about 5 g selected for one analysis	water samples and real tissue samples (muscle tissue of bighead carp)	PS, PMMA	the tissues immersed in 10 % KOH, and the temperature maintained at 60 °C for 36 h; Raman spectroscopy: integration time of 50 s	(Li et al., 2022)
SEM/CL		consumer plastics (bottles, bags, cables, teabags, boxes, cups, etc.)	HDPE, LDPE, PA, PP, PS and PET	typical integration times of 200 ms/pixel and 400 ms/pixel applied.	(Höppener et al., 2023)

Blair et al. studied the distribution of microscopic debris in an urban river near the marine environment in the Western Scotland to assess the concentration and distribution of primary and secondary MPs (sized 2.8 mm–11 μm), using light and SEM-EDS (Blair et al., 2019). In this study, bank sediment samples were collected by the authors from a site representing of sediment accumulation in the River Kelvin located in the west end of Glasgow (Scotland), close to its discharge to the Clyde estuary, and were fractionated based on size and processed for the extraction of MPs by density separation. Total abundances were found to be 161–432 MPs kg^{-1} dry sediment, with fibres as the dominant type, comprising >88 % of total counts. In this study, SEM-EDS facilitated a fast screening of plastic vs non-plastic pellets, and improved the identification of smaller fragments, with certain limitations. Using a similar methodology based on SEM-EDS, others studied the presence of MPs in regurgitated pellets of the common kingfisher (*Alcedo atthis*) sampled along the Ticino River (North Italy). Plastic elements from these samples were detected and identified by visual inspection prior to μ–FTIR and SEM–EDS. Overall, authors found 12 MPs from at least 3 different polymers in 7.5 % of the pellets. Authors stated that by applying high-resolution imaging by SEM–EDS, they were able to confirm the prevalence of ingested fibres that are otherwise not easily detectable under stereo or binocular microscopes (Winkler et al., 2020).

6.2. *SEM coupled with surface–enhanced Raman spectroscopy*

Li et al. used SEM coupled with SERS to determine MNPs in water samples and in real tissue samples (muscle tissue of bighead carp) (Li et al., 2022). This method combined the advantages of ultrahigh spatial resolution of SEM technique and structural fingerprint of Raman spectroscopy, as mentioned in previous parts. Using this method, authors were able to observe single MNPs of PS and PMMA in samples studied.

6.3. *SEM combined with cathodoluminescence*

Höppener et al. reported a proof-of-concept study combining SEM with cathodoluminescence (CL) to show that 6 of the most frequently found plastics (HDPE, LDPE, PA, PP, PS and PET) have unique spectra which could enable the identification of the smallest MNPs (Höppener et al., 2023). They first built a spectral database with 111 plastic samples from reference and consumer plastics having different sizes (0.001–1 mm), colors and shapes (such as irregular, fibre, spheres). Later, authors trained multiple machine learning (ML) classification models using an Artificial Neural Network approach in order to predict plastic type given the CL spectra of those plastics. Using these classification models, they could classify these plastics, including even difficult samples such as black colored plastics, based on their CL spectra with 97 % accuracy, proving that this method is robust towards differences in the samples. Since most misclassifications occurred between LDPE and HDPE in their study, a separate model for LDPE and HDPE allowed for over 99 % accuracy for the classification of HDPE and LDPE with the use of a two-step approach (Höppener et al., 2023). Moreover, authors stated that the developed model is promising in terms of the identification and classification of MNPs which are too small for other conventional methods including μ-FTIR and μ-Raman.

Table 1 summarizes methodologies covered in this review in terms of the amount of the sample needed, origin of environmental water samples to be analyzed (or the type of aquatic organisms), the types of MNPs studied/characterized and certain experimental time variables. These parameters have not been reported in all studies covered, thus included in the table only if reported. Please also note that there are other studies reporting on different MNPs analysis techniques, which have not been covered in the present review, due to limited availability of space.

7. Conclusion

In this review, we covered and critically discussed the methods developed using various techniques recommended for the determination of MNPs in different water samples from seawater to wastewater. Their sensitive and selective detection and quantification, especially in the aquatic environments, is of high importance. As reported in the

literature, particularly spectroscopic methods, chromatographic methods and scanning electron microscopy have been used successfully for the determination of MNPs in various water environments. Method development studies for the determination of MNPs in diverse samples continue to be carried out increasingly. Although many improvements have been made in the methodologies for MNPs analysis in recent years as also reported here, many methods developed for the determination of MNPs still have their own shortcomings in the practical applications, and there is no validated analytical method for MNPs determination. Moreover, the use of a single method may not always result in a complete information on MNPs present in analyzed samples. Besides, using a single method for MNPs analysis is highly susceptible to interference from false negative or false positive signals, thus reducing the accuracy and reliability of MNPs determination. In order to ensure the accuracy of data obtained on MNPs, multiple methodologies (as we covered in this review, such as the combined use of SEM and Raman methods) can be used in combination to analyze MNPs in diverse environmental samples (Shim et al., 2017; Fang et al., 2023). The more common use of advanced AI algorithms will also certainly improve the prediction of MNPs and decrease the time required for such analyses from experimental data (such as those obtained from TGA–DSC) in near future. It should also be highlighted here that more standardization in all the steps (from sampling to characterization) of MNPs determination is required to improve transparency, reproducibility, and robustness of the findings, thereby increasing the credibility and impact of this research area (Thaiba et al., 2023). Currently available MNPs analysis methods require skilled manpower, are costly, not suited for on-site testing and time-inefficient; therefore, novel methods that can overcome these limitations and suitable for on-site analysis would be highly important, considering the fact that MNPs in a sample of interest can change significantly over time and that MNPs pollution might be even higher in resource-limited areas (Hu et al., 2024). Lastly, based on the full range of MNPs in terms of many physical parameters, publicly available open access database libraries of both spectral and mass information must be established, allowing the accurate analysis of different MNPs present in much more complex environmental systems. In this respect, the use of chemometrics might also be useful, and this will also improve the performance of AI tools used in the determination of MNPs in environmental samples in the near future.

In conclusion, considering a very recent study reporting that microplastics are present in all canine and human testes samples studied (using Pyr–GC/MS), with levels of 122.63 μg/g and 328.44 μg/g, respectively (with PE being dominant), and an observation that a negative correlation is present between specific polymers such as PVC and PET and the normalized weight of the testis, with potential consequences on male reproductive system and male fertility; it is of critical importance to control environmental levels of MNPs contamination with improved identification, quantification, monitoring, mitigation and remediation strategies to minimize the health risks associated with MNPs (Berkel and Özbek, 2024; Hu et al., 2024).

CRediT authorship contribution statement

Caglar Berkel: Writing – original draft, Investigation, Formal analysis. **Oguz Özbek:** Writing – original draft, Investigation, Formal analysis.

Declaration of competing interest

The authors declare that there is no conflict of interest.

References

Andrady, A.L., 2011. Microplastics in the marine environment. Mar. Pollut. Bull. 62 (8), 1596–1605. https://doi.org/10.1016/j.marpolbul.2011.05.030.

Beattie, J.R., McGarvey, J.J., Stitt, A.W., 2023. Raman spectroscopy for the detection of AGEs/ALEs. In: Galluzzi, L., Vitale, I., Kepp, O., Kroemer, G. (Eds.), Raman spectroscopy for the detection of AGEs/ALEs. Cell Senescence. Methods in Molecular Biology, Vol 965. https://doi.org/10.1007/978-1-62703-239-1_20.

Becker, R., Altmann, K., Sommerfeld, T., Braun, U., 2020. Quantification of microplastics in a freshwater suspended organic matter using different thermoanalytical methods – outcome of an interlaboratory comparison. J. Anal. Appl. Pyrolysis 148, 104829. https://doi.org/10.1016/j.jaap.2020.104829.

Berkel, C., Özbek, O., 2024. The mitigation and remediation of micro(nano)plastics to improve environmental and public health. S. Afr. J. Chem. Eng. 48, 194–195. https://doi.org/10.1016/j.sajce.2024.02.003.

Blair, R.M., Waldron, S., Phoenix, V.R., Gauchotte-Lindsay, C., 2019. Microscopy and elemental analysis characterisation of microplastics in sediment of a freshwater urban river in Scotland, UK. Environ. Sci. Pollut. Res. 26, 12491–12504. https://doi.org/10.1007/s11356-019-04678-1.

Castelvetro, V., Corti, A., Biale, G., Ceccarini, A., Degano, I., Nasa, J.La, Lomonaco, T., Manariti, A., Manco, E., Modugno, F., Vinciguerra, V., 2021. New methodologies for the detection, identification, and quantification of microplastics and their environmental degradation by-products. Environ. Sci. Pollut. Res. 28, 46764–46780. https://doi.org/10.1007/s11356-021-12466-z.

Castelvetro, V., Corti, A., Bianchi, S., Ceccarini, A., Manariti, A., Vinciguerra, V., 2020. Quantification of poly (ethylene terephthalate) micro-and nanoparticle contaminants in marine sediments and other environmental matrices. J. Hazar. Mater. 385, 121517. https://doi.org/10.1016/j.jhazmat.2019.121517.

Chen, Y., Wen, D., Pei, J., Fei, Y., Ouyang, D., Zhang, H., Luo, Y., 2020. Identification and quantification of microplastics using Fourier-transform infrared spectroscopy: current status and future prospects. Curr. Opin. Environ. Sci. 18, 14–19. https://doi.org/10.1016/j.coesh.2020.05.004.

Dąbrowska, A., Mielańczuk, M., Syczewski, M., 2022. The Raman spectroscopy and SEM/EDS investigation of the primary sources of microplastics from cosmetics available in Poland. Chemosphore 308, 136407. https://doi.org/10.1016/j.chemosphere.2022.136407.

David J, S.Z., Kucerik J, S.G., 2018. Quantitative analysis of poly(ethylene terephthalate) microplastics in soil via thermogravimetry-mass spectrometry. Anal. Chem. 90, 8793–8799. https://doi.org/10.1021/acs.analchem.8b00355.

Dobrzyniewski, D., Szulczyński, B., Dymerski, T., Gębicki, J., 2021. Development of gas sensor array for methane reforming process monitoring. Sensors 21, 4983. https://doi.org/10.3390/s21154983.

Dümichen, E., Barthel, A.-K., Braun, U., Bannick, C.G., Brand, K., Jekel, M., Senz, R., 2015. Analysis of polyethylene microplastics in environmental samples, using a thermal decomposition method. Water Res 85, 451–457. https://doi.org/10.1016/j.watres.2015.09.002.

Dümichen, E., Eisentraut, P., Celina, M., Braun, U., 2019. Automated thermal extraction-desorption gas chromatography mass spectrometry: a multifunctional tool for comprehensive characterization of polymers and their degradation products. J. Chromatogr. A 1592, 133–142. https://doi.org/10.1016/j.chroma.2019.01.033.

Fabbri, D., 2001. Use of pyrolysis-gas chromatography/mass spectrometry to study environmental pollution caused by synthetic polymers: a case study: the Ravenna Lagoon. J. Anal. Appl. Pyrolysis. 58–59, 361–370. https://doi.org/10.1016/S0165-2370(00)00170-4.

Fang, C., Luo, Y., Chuah, C., Naidu, R., 2023a. Identification of microplastic fibres released from COVID-19 test swabs with Raman imaging. Environ. Sci. Eur. 35, 34. https://doi.org/10.1186/s12302-023-00737-035.

Fang, C., Luo, Y., Naidu, R., 2023b. Microplastics and nanoplastics analysis: options, imaging, advancements and challenges. TrAC, Trends Anal. Chem. 166, 117158. https://doi.org/10.1016/j.trac.2023.117158.

Feng, Y., Tu, C., Li, R., Wu, D., Yang, J., Xia, Y., Peijnenburg, W.J.G.M., Luo, Y., 2023. A systematic review of the impacts of exposure to micro- and nano-plastics on human tissue accumulation and health. Eco-Environ. Heal. 2, 195–207. https://doi.org/10.1016/j.eehl.2023.08.002.

Fries, E., Dekiff, J.H., Willmeyer, J., Nuelle, M.T., Ebert, M., Remy, D., 2013. Identification of polymer types and additives in marine microplastic particles using pyrolysis-GC/MS and scanning electron microscopy. Environ. Sci.: Processes Impacts 15, 1949–1956. https://doi.org/10.1039/C3EM00214D.

Funck, M., Al-Azzawi, M.S.M., Yildirim, A., Knoop, O., Schmidt, T.C., Drewes, J.E., Tuerk, J., 2021. Release of microplastic particles to the aquatic environment via wastewater treatment plants: the impact of sand filters as tertiary treatment. Chem. Eng. J. 426, 130933. https://doi.org/10.1016/j.cej.2021.130933.

Furfaro, G., D'Elia, M., Mariano, S., Trainito, E., Solca, M., Piraino, S., Belmonte, G., 2022. SEM/EDX analysis of stomach contents of a sea slug snacking on a polluted seafloor reveal microplastics as a component of its diet. Sci. Rep. 12, 10244. https://doi.org/10.1038/s41598-022-14299-3.

Gaba, F., Tipping, W.J., Salji, M., Faulds, K., Graham, D., Leung, H.Y., 2022. Raman spectroscopy in prostate cancer: techniques, applications and advancements. Cancers (Basel) 14, 1535. https://doi.org/10.3390/cancers14061535.

Gillibert, R., Balakrishnan, G., Deshoules, Q., Tardivel, M., Magazzù, A., et al., 2019. Raman tweezers for small microplastics and nanoplastics identification in seawater. Environ. Sci. Technol. 53, 9003–9013. https://doi.org/10.1021/acs.est.9b03105.

Han, X.X., Rodriguez, R.S., Haynes, C.L., et al., 2021. Surface-enhanced Raman spectroscopy. Nat. Rev. Methods Primers 1, 87. https://doi.org/10.1038/s43586-021-00083-6.

Harrison, J.P., Ojeda, J.J., Romero-Gonzalez, M.E., 2012. The applicability of reflectance micro-Fourier-transform infrared spectroscopy for the detection of synthetic microplastics in marine sediments. Sci. Total. Environ. 416, 455–463. https://doi.org/10.1016/j.scitotenv.2011.11.078.

He, S., Jia, M., Xiang, Y., Song, B., Xiong, W., Cao, J., Peng, H., Yang, Y., Wang, W., Yang, Z., Zeng, G., 2022. Biofilm on microplastics in aqueous environment:

physicochemical properties and environmental implications. J. Hazard. Mater. 424, 127286. https://doi.org/10.1016/j.jhazmat.2021.127286.
Hermabessiere, L., Himber, C., Boricaud, B., Kazour, M., Amara, R., Cassone, A.-L., Laurentie, M., Paul-Pont, I., Soudant, P., Dehaut, A., Duflos, G., 2018. Optimization, performance, and application of a pyrolysis-GC/MS method for the identification of microplastics. Anal. Bioanal. Chem. 410, 6663–6676. https://doi.org/10.1007/s00216-018-1279-0.
Höppener, E.M., Shahmohammadi, M.S., Parker, L.A., Henke, S., Urbanus, J.H., 2023. Classification of (micro) plastics using cathodoluminescence and machine learning. Talanta 253, 123985. https://doi.org/10.1016/j.talanta.2022.123985.
Hu, C.J., Garcia, M.A., Nihart, A., Liu, R., Yin, L., Adolphi, N., Gallero, D.F., Kang, H., Campen, M.J., Yu, X., 2024. Microplastic presence in dog and human testis and its potential association with sperm count and weights of testis and epididymis. Toxicol. Sci. kfae060. https://doi.org/10.1093/toxsci/kfae060.
Huang, D., Tao, J., Cheng, M., Deng, R., Chen, S., Yin, L., Li, R., 2021. Microplastics and nanoplastics in the environment: macroscopic transport and effects on creatures. J. Hazard. Mater. 407, 124399. https://doi.org/10.1016/j.jhazmat.2020.124399.
Ishimura, T., Iwai, I., Matsui, K., Mattonai, M., Watanabe, A., Robberson, W., Cook, A.-M., Allen, H.L., Pipkin, W., Teramae, N., Ohtani, H., Watanabe, C., 2021. Qualitative and quantitative analysis of mixtures of microplastics in the presence of calcium carbonate by pyrolysis-GC/MS. J. Anal. Appl. Pyrol. 157, 10518.
Issac, M.N., Kandasubramanian, B., 2021. Effect of microplastics in water and aquatic systems. Environ. Sci. Pollut. Res. Int. 28, 19544–19562. https://doi.org/10.1007/s11356-021-13184-2.
Käppler, A., Windrich, F., Löder, M.G., Malanin, M., Fischer, D., Labrenz, M., Eichhorn, K.-J., Voit, B., 2015. Identification of microplastics by FTIR and Raman microscopy: a novel silicon filter substrate opens the important spectral range below 1300 cm^{-1} for FTIR transmission measurements. Anal. Bioanal. Chem. 407, 6791–6801. https://doi.org/10.1007/s00216-015-8850-8.
Kniggendorf, A.K., Wetzel, C., Roth, B., 2019. Microplastics detection in streaming tap water with Raman spectroscopy. Sensors 19, 1839. https://doi.org/10.3390/s19081839.
Li, G., Yang, Z., Pei, Z., Li, Y., Yang, R., Liang, Y., Zhang, Q., Jiang, G., 2022. Single-particle analysis of micro/nanoplastics by SEM-Raman technique. Talanta 249, 123701. https://doi.org/10.1016/j.talanta.2022.123701.
Li, Z., Han, K., Zhang, A., Wang, T., Yan, Z., Ding, Z., Shen, Y., Zhang, M., Zhang, W., 2024. Honeycomb-like AgNPs@TiO_2 array SERS sensor for the quantification of micro/nanoplastics in the environmental water samples. Talanta 266, 125070. https://doi.org/10.1016/j.talanta.2023.125070.
Lim, S.J., Park, Y.K., Kim, H., Kwon, J., Moon, H.M., Lee, Y., A.Watanabe, N.Teramae, Ohtani, H., Kim, Y.M., 2022. Selective solvent extraction and quantification of synthetic microfibers in textile laundry wastewater using pyrolysis-gas chromatography/mass spectrometry. J. Chem. Eng. 434, 134653. https://doi.org/10.1016/j.cej.2022.134653.
Lin, Y., Huang, X., Liu, Q., Lin, Z., Jiang, G., 2020. Thermal fragmentation enhanced identification and quantification of polystyrene micro/nanoplastics in complex media. Talanta 208, 120478. https://doi.org/10.1016/j.talanta.2019.120478.
Liu, W., Liao, H., Wei, M., Junaid, M., Chen, G., Wang, J., 2022. Effects of plastic particles on aquatic invertebrates and fish – a review. Environ. Toxicol. Pharmacol. 96, 104013. https://doi.org/10.1016/j.etap.2022.104013.
Liu, W., Liao, H., Wei, M., Junaid, M., Chen, G., Wang, J., 2024b. Biological uptake, distribution and toxicity of micro(nano)plastics in the aquatic biota: a special emphasis on size-dependent impacts. TrAC, Trends Anal. Chem. 170, 117477. https://doi.org/10.1016/j.trac.2023.117477.
Liu, W., Liao, H., Wei, M., Junaid, M., Chen, G., Wang, J., 2024a. Biological uptake, distribution and toxicity of micro (nano) plastics in the aquatic biota: a special emphasis on size-dependent impacts. TrAC, Trends Anal. Chem. 170, 117477. https://doi.org/10.1016/j.trac.2023.117477.
Liu, Y., Li, R., Yu, J., Ni, F., Sheng, Y., Scircle, A., Cizdziel, J.V., Zhou, Y., 2021. Separation and identification of microplastics in marine organisms by TGA-FTIR-GC/MS: a case study of mussels from coastal China. Environ. Pollut. 272, 115946. https://doi.org/10.1016/j.envpol.2020.115946.
Loder, M., Kuczera, M., Mintenig, S., Lorenz, C., Gerdts, G., 2015. Focal plane array detector-based micro-Fourier-transform infrared imaging for the analysis of microplastics in environmental samples. Environ. Chem. 12, 563–581.
Ma, Y.B., Xie, Z.Y., Hamid, N., Tang, Q.P., Deng, J.Y., Luo, L., Pei, D.S., 2023. Recent advances in micro (nano) plastics in the environment: distribution, health risks, challenges and future prospects. Aquat. Toxicol. 261, 106597. https://doi.org/10.1016/j.aquatox.2023.106597.
Majewsky, M., Bitter, H., Eiche, E., Horn, H., 2016. Determination of microplastic polyethylene (PE) and polypropylene (PP) in environmental samples using thermal analysis (TGA-DSC). Sci. Total Environ. 568, 507–511. https://doi.org/10.1016/j.scitotenv.2016.06.017.
Miserli, K., Lykos, C., Kalampounias, A.G., Konstantinou, I., 2023. Screening of microplastics in aquaculture systems (Fish, Mussel, and Water Samples) by FTIR, scanning electron microscopy–energy dispersive spectroscopy and micro-raman spectroscopies. App. Sci. 13, 9705. https://doi.org/10.3390/app13179705.
Morgado, V., Gomes, L., da Silva, R.J.B., Palma, C., 2021. Validated spreadsheet for the identification of PE, PET, PP and PS microplastics by micro-ATR-FTIR spectra with known uncertainty. Talanta 234, 122624. https://doi.org/10.1016/j.talanta.2021.122624.
Müller, A., Goedecke, C., Eisentraut, P., Piechotta, C., Braun, U., 2020. Microplastic analysis using chemical extraction followed by LC-UV analysis: a straightforward approach to determine PET content in environmental samples. Environ. Sci. Eur. 32, 85. https://doi.org/10.1186/s12302-020-00358-x.
Munoz, L.P., Baez, A.G., McKinney, D., Garelick, H., 2018. Characterisation of "flushable" and "non-flushable" commercial wet wipes using microRaman, FTIR spectroscopy and fluorescence microscopy: to flush or not to flush. Environ. Sci. Pollut. Res. 25, 20268–20279. https://doi.org/10.1007/s11356-018-2400-9.
N'cho, J.S., Fofana, I., Hadjadj, Y., Beroual, A., 2016. Review of physicochemical-based diagnostic techniques for assessing insulation condition in aged transformers. Energies 9, 367. https://doi.org/10.3390/en9050367.
Nel, H.A., Chetwynd, A.J., Kelly, C.A., Stark, C., Valsami-Jones, E., Krause, S., Lynch, I., 2021. An untargeted thermogravimetric analysis-fourier transform infrared-gas chromatography-mass spectrometry approach for plastic polymer identification. Environ. Sci. Technol. 55, 8721–8729. https://doi.org/10.1021/acs.est.1c01085.
Nuelle, M.T., Dekiff, J.H., Remy, D., Fries, E., 2014. A new analytical approach for monitoring microplastics in marine sediments. Environ. Poll. 184, 161–169. https://doi.org/10.1016/j.envpol.2013.07.027.
Okoffo, E.D., Thomas, K.V., 2024. Quantitative analysis of nanoplastics in environmental and potable waters by pyrolysis-gas chromatography–mass spectrometry. J. Hazard. Mater. 464, 133013. https://doi.org/10.1016/j.jhazmat.2023.133013.
Osman, A.I., Hosny, M., Eltaweil, A.S., et al., 2023. Microplastic sources, formation, toxicity and remediation: a review. Environ. Chem. Lett. 21, 2129–2169. https://doi.org/10.1007/s10311-023-01593-3.
Primpke, S., Fischer, M., Lorenz, C., Gerdts, G., Scholz-Böttcher, B.M., 2020. Comparison of pyrolysis gas chromatography/mass spectrometry and hyperspectral FTIR imaging spectroscopy for the analysis of microplastics. Anal. Bioanal. Chem. 412, 8283–8298. https://doi.org/10.1007/s00216-020-02979-w.
Primpke, S., Lorenz, C., Rascher-Friesenhausen, R., Gerdts, G., 2017. An automated approach for microplastics analysis using focal plane array (FPA) FTIR microscopy and image analysis. Anal. Methods 9, 1499–1511. https://doi.org/10.1039/C6AY02476A.
Qi, G., Zhao, L., Liu, J., Tian, C., Zhang, S., 2024. Single particle detection of micro/nano plastics based on recyclable SERS sensor with two-dimensional AuNPs thin films. Mater. Today Commun. 38, 108293. https://doi.org/10.1016/j.mtcomm.2024.108293.
Rathore, C., Saha, M., Gupta, P., Kumar, M., Naik, A., de Boer, J., 2023. Standardization of micro-FTIR methods and applicability for the detection and identification of microplastics in environmental matrices. Sci. Total Environ. 888, 164157. https://doi.org/10.1016/j.scitotenv.2023.164157.
Ravit, B., Cooper, K., Moreno, G., Buckley, B., Yang, I., Deshpande, A., Meola, S., Jones, D., Hsieh, A., 2017. Microplastics in urban New Jersey freshwaters: distribution, chemical identification, and biological affects. AIMS Environ. Sci. 4, 809–826. https://doi.org/10.3934/environsci.2017.6.809.
Renner, G., Sauerbier, P., Schmidt, T.C., Schram, J., 2019. Robust automatic identification of microplastics in environmental samples using FTIR microscopy. Anal. Chem. 91, 9656–9664. https://doi.org/10.1021/acs.analchem.9b01095.
Ribeiro, F., Okoffo, E.D., O'Brien, J.W., Fraissinet-Tachet, S., O'Brien, S., Gallen, M., Samanipour, S., Kaserzon, S., Mueller, J.F., Galloway, T., Thomas, K.V., 2020. Quantitative analysis of selected plastics in high-commercial-value Australian seafood by pyrolysis gas chromatography mass spectrometry. Environ. Sci. Technol. 54, 9408–9417. https://doi.org/10.1021/acs.est.0c02337.
Ribeiro-Claro, P., Nolasco, M.M., Araújo, C., 2017. Characterization of microplastics by Raman spectroscopy. Compr. Anal. Chem. 75, 119–151. https://doi.org/10.1016/bs.coac.2016.10.001.
Rodrigues, M.O., Abrantes, N., Gonçalves, F.J.M., Nogueira, H., Marques, J.C., Gonçalves, A.M.M., 2019. Impacts of plastic products used in daily life on the environment and human health: what is known? Environ. Toxicol. Pharmacol. 72, 103239. https://doi.org/10.1016/j.etap.2019.103239.
Santos, L.H., Insa, S., Arxé, M., Buttiglieri, G., Rodríguez-Mozaz, S., Barceló, D., 2023. Analysis of microplastics in the environment: identification and quantification of trace levels of common types of plastic polymers using pyrolysis-GC/MS. MethodsX 10, 102143. https://doi.org/10.1016/j.mex.2023.102143.
Schell, T., Hurley, R., Nizzetto, L., Rico, A., Vighi, M., 2021. Spatio-temporal distribution of microplastics in a Mediterranean river catchment: the importance of wastewater as an environmental pathway. J. Hazard. Mater. 420, 126481. https://doi.org/10.1016/j.jhazmat.2021.126481.
Schwaferts, C., Niessner, R., Elsner, M., Ivleva, N.P., 2019. Methods for the analysis of submicrometer- and nanoplastic particles in the environment. TrAC, Trends Anal. Chem. 112, 52–65. https://doi.org/10.1016/j.trac.2018.12.014.
Selamat, J., Rozani, N.A.A., Murugesu, S., 2021. Application of the metabolomics approach in food authentication. Molecules 26, 7565. https://doi.org/10.3390/molecules26247565.
Shim, W.J., Hong, S.H., Eo, S.E., 2017. Identification methods in microplastic analysis: a review. Anal. Methods 9, 1384–1391. https://doi.org/10.1039/C6AY02558G.
Sullivan, G.L., Gallardo, J.D., Jones, E.W., Hollliman, P.J., T.M, Watson, Sarp, S., 2020. Detection of trace sub-micron (nano) plastics in water samples using pyrolysis-gas chromatography time of flight mass spectrometry (PY-GCToF). Chemosphere 249, 126179. https://doi.org/10.1016/j.chemosphere.2020.126179.
Szymańska, M., Obolewski, K., 2020. Microplastics as contaminants in freshwater environments: a multidisciplinary review. Ecohydrol. Hydrobiol. 20, 333–345. https://doi.org/10.1016/j.ecohyd.2020.05.001.
Tagg, A.S., Sapp, M., Harrison, J.P., Ojeda, J.J., 2015. Identification and quantification of microplastics in wastewater using focal plane array-based reflectance micro-FT-IR imaging. Anal. Chem. 87, 6032–6040. https://doi.org/10.1021/acs.analchem.5b00495.
Tan, X., Yu, X., Cai, L., Wang, J., Peng, J., 2019. Microplastics and associated PAHs in surface water from the Feilaixia Reservoir in the Beijiang River, China. Chemosphere 221, 834–840. https://doi.org/10.1016/j.chemosphere.2019.01.022.

Thaiba, B.M., Sedai, T., Bastakoti, S., Karki, A., Anuradha, K.C., Khadka, G., Acharya, S., Kandel, B., Giri, B., Neupane, B.B., 2023. A review on analytical performance of micro-and nanoplastics analysis methods. Arab. J. Chem. 16, 104686. https://doi.org/10.1016/j.arabjc.2023.104686.

Thompson, R.C., Olson, Y., Mitchell, R.P., Davis, A., Rowland, S.J., John, A.W.G., McGonigle, D., Russell, A.E., 2004. Lost at sea: where is all the plastic? Science 80, 838. https://doi.org/10.1126/science.1094559.

Tian, L., Skoczynska, E., Siddhanti, D., van Putten, R.J., Leslie, H.A., Gruter, G.J.M., 2022. Quantification of polyethylene terephthalate microplastics and nanoplastics in sands, indoor dust and sludge using a simplified in-matrix depolymerization method. Mar. Pollut. Bull. 175, 113403. https://doi.org/10.1016/j.marpolbul.2022.113403.

Umaru, I.J., Emmanuel, A.N.J., Habibu, B., Umaru, K.I., Chizaram, B.C., 2019. Toxicity and environmental plastic disposal, its death and survival rate. Int. J. Adv. Chem. Res. 3, 64–75. https://doi.org/10.33545/26174693.2019.v3.i2a.136.

Vianello, A., Jensen, R.L., Liu, L., Vollertsen, J., 2019. Simulating human exposure to indoor airborne microplastics using a Breathing Thermal Maniki. Sci. Rep. 9, 8670. https://doi.org/10.1038/s41598-019-45054-w.

Vilakati, B., Sivasankar, V., Nyoni, H., Mamba, B.B., Omine, K., Msagati, T.A., 2021. The Py–GC-TOF-MS analysis and characterization of microplastics (MPs) in a wastewater treatment plant in Gauteng Province, South Africa. Ecotoxicol. Environ. Saf. 222, 112478. https://doi.org/10.1016/j.ecoenv.2021.112478.

Vonderach, T., Gundlach-Graham, A., Günther, D., 2023. Determination of carbon in microplastics and single cells by total consumption microdroplet ICP-TOFMS. Anal. Bioanal. Chem. https://doi.org/10.1007/s00216-023-05064-0.

Wang, H., Wang, Q., Lv, M., Li, J., Zhao, X., Song, Z., Wang, X., You, J., Wang, Y., Chen, L., 2023. Marine micro(nano)plastics determination and its environmental toxicity evaluation. TrAC, Trends Anal. Chem. 168, 117332. https://doi.org/10.1016/j.trac.2023.117332.

Winkler, A., Nessi, A., Antonioli, D., Laus, M., Santo, N., Parolini, M., Tremolada, P., 2020. Occurrence of microplastics in pellets from the common kingfisher (Alcedo atthis) along the Ticino River, North Italy. Environ. Sci. Pollut. Res. 27, 41731–41739. https://doi.org/10.1007/s11356-020-10163-x.

Wright, S.L., Thompson, R.C., Galloway, T.S., 2013. The physical impacts of microplastics on marine organisms: a review. Environ. Poll. 178, 483–492. https://doi.org/10.1016/j.envpol.2013.02.031.

Wu, P., Tang, Y., Cao, G., Li, J., Wang, S., Chang, X., Dang, M., Jin, H., Zheng, C., Cai, Z., 2020. Determination of environmental micro(nano)plastics by matrix-assisted laser desorption/ionization– time-of-flight mass spectrometry. Anal. Chem. 92, 14346–14356. https://doi.org/10.1021/acs.analchem.0c01928.

Wu, P., Wu, X., Huang, Q., Yu, Q., Jin, H., Zhu, M., 2023b. Mass spectrometry-based multimodal approaches for the identification and quantification analysis of microplastics in food matrix. Front. Nutr. 10, 1163823. https://doi.org/10.3389/fnut.2023.1163823.

Wu, P., Wu, X., Huang, Q., Yu, Q., Jin, H., Zhu, M., 2023a. Mass spectrometry-based multimodal approaches for the identification and quantification analysis of microplastics in food matrix. Front. Nutr. 10, 1163823. https://doi.org/10.3389/fnut.2023.1163823.

Wu, Q., Xiao, D., Wang, N., Masia, F., Langbein, W., Li, B., 2024. Rapid identification of micro and nanoplastics by line scan Raman micro-spectroscopy. Talanta 266, 125067. https://doi.org/10.1016/j.talanta.2023.125067.

Xu, Y., Ou, Q., Wang, X., Hou, F., Li, P., van der Hoek, J.P., Liu, G., 2023. Assessing the mass concentration of microplastics and nanoplastics in wastewater treatment plants by pyrolysis gas chromatography–mass spectrometry. Environ. Sci. Technol. 57, 3114–3123. https://doi.org/10.1021/acs.est.2c07810.

Yakovenko, N., Carvalho, A., ter Halle, A., 2020. Emerging use thermo-analytical method coupled with mass spectrometry for the quantification of micro (nano) plastics in environmental samples. TrAC, Trends Anal. Chem. 131, 115979. https://doi.org/10.1016/j.trac.2020.115979.

Yee, M., Hii, L., Looi, C., Lim, W., Wong, S., Kok, Y., Tan, B., Wong, C., Leong, C., 2021. Impact of microplastics and nanoplastics on human health. Nanomaterials 11, 496. https://doi.org/10.3390/nano11020496.

Yu, Z., Xu, X., Guo, L., Yuzuak, S., Lu, Y., 2024. Physiological and biochemical effects of polystyrene micro/nano plastics on *Arabidopsis thaliana*. J. Hazard. Mater., 133861 https://doi.org/10.1016/j.jhazmat.2024.133861.

Yurtsever, M., 2023. Microplastics: an overview. DEU FMD 17 (50), 68–83.

Yuvedha, S., Yoganandhan, U., Nampoothiri, N.V.N., 2019. Quantitative analysis of microplastics in wastewater from treatment plant by visual identification and FT-IR imaging using H_2O_2 and $FeSO_4$: a case study. IOP Conf. Ser.: Mater. Sci. Eng. 561, 012026. https://doi.org/10.1088/1757-899X/561/1/012026.

Zangmeister, C.D., Radney, J.G., Benkstein, K.D., Kalanyan, B., 2022. Common single-use consumer plastic products release trillions of sub-100 nm nanoparticles per liter into water during normal use. Environ. Sci. Technol. 56, 5448. https://doi.org/10.1021/acs.est.1c06768.

Zhang, J., Fu, D., Feng, H., Li, Y., Zhang, S., Peng, C., Wang, Y., Sun, H., Wang, L., 2024. Mass spectrometry detection of environmental microplastics: advances and challenges. TrAC, Trends Anal. Chem. 170, 117472. https://doi.org/10.1016/j.trac.2023.117472.